

# A Novel CFD Scheme for Collision of Micro-bubbles in Turbulent Flow

Arman Raoufi, Mehrzad Shams, and Reza Ebrahimi

**Abstract**— A numerical scheme for bubble trajectories including their collisions is developed. An Eulerian-Lagrangian computational scheme is used to study the bubble trajectories. The 2D averaged Navier Stokes equations are solved. The SIMPLEC algorithm is used to relate the pressure to velocity. A one-way coupling is assumed and the effects of the bubbles on carrier flow are neglected. The bubble equation of motion includes the drag, buoyancy, pressure gradient, Saffman lift and bubble volume change forces. The variation of the bubble radius is modelled using the Rayleigh-Plesset equation. The Kraichnan model is used to simulate the instantaneous turbulence fluctuation velocities. The hard sphere collision model is used to model the bubble collisions and the effects of bubble rotations are neglected. Trajectories of micro-bubbles in the near wall region are investigated, and the rate of collisions and bubble settling are studied. The results are compared with other simulations and good agreement is observed.

**Index Terms**—CFD, Two phase flow, Bubble, Collision.

## I. INTRODUCTION

Bubble dynamics has been the subject of intensive theoretical and experimental studies since Lord Raleigh (1917) found the well-known analytic solution of this problem for inviscid liquids. Plesset developed Rayleigh works and obtained a famous equation for bubble radius, known as Rayleigh – Plesset (RP) equation [1]. The RP equation described the dynamics of a spherical void or gas bubble in viscous liquids and is also used as a first approximation in more complex problem such as cavitation near solid boundaries.

Bubbly flow could be analyzed as two fluids in the Eulerian/Eulerian approach, or as a continuum phase and another bubble phase in the Eulerian/Lagrangian or trajectory approach. The bubble equation of motion is solved simultaneously with the RP equation to determine its trajectory (Eulerian/Lagrangian method).

Meyer et al. developed a computer code to model bubble trajectory, consisting of a numerical solution to the RP

equation coupled to a set of trajectory equations [2]. Using the code, trajectories and growths were computed for bubble of varying initial sizes.

Hsiao and Pauley completed a Reynolds-averaged Navier-Stokes computation of a tip vortex flow from a finite-span hydrofoil [3]. The Rayleigh-Plesset equation for bubble growth was coupled with Johnson and Hsieh's [4] trajectory equation to track single microbubbles through the steady-state flow field and thereby infer cavitation inception.

Farrell developed an Eulerian/Lagrangian computational procedure for the prediction of the cavitation inception [5]. The trajectories were computed using Newton's second law with models for various forces acting on the bubble. The growth was modeled using RP equation.

Raoufi et al. used the Eulerian/Lagrangian approach to simulate micro bubble trajectory in a gate slot of dam [6].

In works mentioned above, collision of bubbles was ignored. Since direct simulation of particle, droplet and bubble collisions is associated with significant increase in the computational cost, many models for collision were proposed in the literature. Dukowicz simulated droplets collision by using the representative particle technique [7]. O'Rourke proposed an algorithm for collisions in sprays that is widely used in commercial CFD codes [8]. O'Rourke's method was based on a stochastic estimation of collisions. Sommerfeld and Zivkovic simulated particle motion in pneumatic conveying using particle-particle and particle-wall collision models [9].

Tsuji et al. provided a discrete particle simulation of a two-dimensional fluidized bed using a soft sphere model [10]. In the soft-sphere model, the collisions between particles and between particle and wall were evaluated using Hooke's linear spring and dashpot models. Their model was further modified by Hoomans et al. who developed a new hard sphere collision model, which was used by a number of researchers [11]. Goldschmidt et al. [12] and Lu et al. [13] studied solid particles and bubbles in fluidized bed using discrete hard-sphere model. This model was used to simulate flows in three-phase bubble column by Zhang and Ahmadi [14].

In this study, an Eulerian–Lagrangian method for liquid–gas flows in channel is developed. The channel had a length of 1 m with a width of 0.2 m. Velocity of flow in the channel is considered 20 m/s. In this model, the liquid is the continuous phase and the bubbles are treated as the dispersed discrete phase. The micro bubbles are assumed to remain spherical and their size variations are modelled using the Rayleigh-Plesset equation. The volume-averaged, incompressible Navier–Stokes equation is solved for the liquid phase. The Kraichnan model is used to simulate the

Manuscript received 23 April, 2008.

Arman Raoufi is with Department of Mechanical Engineering, K.N.Toosi University of Technology, Tehran, Iran (e-mail: ar.raoufi@gmail.com).

Mehrzad Shams is with Department of Mechanical Engineering, K.N.Toosi University of Technology, Tehran, Iran (corresponding author to provide phone: +98-912-359-6236; fax: +98-021-733-4338; e-mail: shams@kntu.ac.ir).

Reza Ebrahimi is with Department of Mechanical Engineering, K.N.Toosi University of Technology, Tehran, Iran (e-mail: Ebrahimi@kntu.ac.ir).

instantaneous velocity fluctuations.

The bubble motions are simulated by the Lagrangian trajectory analysis procedure. For dilute bubble volume fractions, the effects of bubbles on the carrier fluid are neglected and a one-way coupling is used. Forces acting on the bubble include drag, buoyancy, pressure gradient, Saffman lift and volume variation. Bubble–bubble collisions are included in the analysis using a hard sphere collision model along the line of Hoomans *et al.* [11]. A test case is used to validate the bubbles collision algorithm. The analytical and numerical results are compared and good agreement was found. A number of micro-bubble are released in the near wall region ( $0 < y^+ < 40$ ) and their trajectories include their collisions are investigated. Rate of collision and settling of bubbles are studied.

## II. FLOW SIMULATION

Since the flow is turbulent, it is important to use an appropriate turbulence model for evaluating the mean flow field. Reynolds stress transport model (RSTM) of Launder *et al.* [15] is used in this study. This model accounts for the evolution of individual turbulence stress components, and is well suited for evaluating anisotropic turbulence stresses that are needed for the present study.

### A. Mean-flow model

For an incompressible fluid flow, the equation of continuity and balance of momentum for the mean motion are given as:

$$\begin{aligned} \frac{\partial \bar{u}_i}{\partial x_i} &= 0 \\ \frac{\partial \bar{u}_i}{\partial t} + \bar{u}_j \frac{\partial \bar{u}_i}{\partial x_j} &= -\frac{1}{\rho} \frac{\partial \bar{p}}{\partial x_i} + \nu \frac{\partial^2 \bar{u}_i}{\partial x_j \partial x_j} - \frac{\partial}{\partial x_j} R_{ij} \end{aligned} \quad (1)$$

Where  $\bar{u}_i$  is the mean velocity,  $x_i$  is the position,  $t$  is the time,  $\bar{p}$  is the mean pressure,  $\rho$  is the constant mass density,  $\nu$  is the kinematic viscosity, and  $R_{ij} = \overline{u'_i u'_j}$  is the Reynolds stress tensor. Here,  $u'_i = u_i - \bar{u}_i$  is the velocity fluctuation component.

The RSTM provides transport equations for evaluation of the turbulence stresses. i.e,

$$\begin{aligned} \frac{\partial}{\partial t} R_{ij} + \bar{u}_k \frac{\partial}{\partial x_k} R_{ij} &= \frac{\partial}{\partial x_k} \left( \frac{\nu_t}{\sigma^k} \frac{\partial}{\partial x_k} R_{ij} \right) - \left[ R_{jk} \frac{\partial \bar{u}_j}{\partial x_k} + R_{jk} \frac{\partial \bar{u}_i}{\partial x_k} \right] \\ &- C_1 \frac{\varepsilon}{k} \left[ R_{ij} - \frac{2}{3} \delta_{ij} P \right] - C_2 \left[ P_{ij} - \frac{2}{3} \delta_{ij} P \right] - \frac{2}{3} \delta_{ij} \varepsilon \end{aligned} \quad (2)$$

Here the turbulence production is defined as,

$$P_{ij} = -R_{jk} \frac{\partial \bar{u}_j}{\partial x_k} - R_{jk} \frac{\partial \bar{u}_i}{\partial x_k}, P = \frac{1}{2} P_{ij} \quad (3)$$

Where  $P$  is the fluctuation kinetic energy production. In Equation (2)  $\nu_t$  is the turbulence (eddy) viscosity; and

$\sigma^k = 1.0, C_1 = 1.8, C_2 = 0.6$  are empirical constants.

The transport equation for the turbulence dissipation rate,  $\varepsilon$ , is given as:

$$\frac{\partial \varepsilon}{\partial t} + \bar{u}_j \frac{\partial \varepsilon}{\partial x_j} = \frac{\partial}{\partial x_i} \left[ \left( \nu + \frac{\nu_t}{\sigma^\varepsilon} \right) \frac{\partial \varepsilon}{\partial x_i} \right] - C^{\varepsilon 1} \frac{\varepsilon}{k} R_{ij} \frac{\partial \bar{u}_i}{\partial x_j} - C^{\varepsilon 2} \frac{\varepsilon^2}{k} \quad (4)$$

Here  $k = \frac{1}{2} \overline{u'_i u'_i}$  is the fluctuation kinetic energy. The values of constants are [15]:

$$\sigma^\varepsilon = 1.3, C^{\varepsilon 1} = 1.44, C^{\varepsilon 2} = 1.92 \quad (5)$$

### B. Velocity Fluctuations

In this study, the Gaussian random field model developed by Kraichnan [16] is used to simulate a homogenous and isotropic pseudo-turbulent flow field. Maxey used the technique earlier to study the gravitational settling of small particles in a randomly fluctuating flow field [17], and Fan and Ahmadi [18] used Kraichnan model to study the turbulent diffusivity of ellipsoidal particles. The expression for the instantaneous velocity field is given by:

$$u_i^* = \sqrt{\frac{2}{N}} \left\{ \sum_{n=1}^N p(k_n) \cos(k_n \cdot x_i^* + \omega_n t^*) + \sum_{n=1}^N q(k_n) \sin(k_n \cdot x_i^* + \omega_n t^*) \right\} \quad (6)$$

where  $p(k_n) = \zeta_n \times k_n$  and  $q(k_n) = \xi_n \times k_n$ . The components of vector  $\zeta$  and  $\xi$  and the frequency  $\omega$  are independent zero mean unit variance Gaussian random variables, while each component of  $k$  is picked from a population of zero mean Gaussian random numbers with a standard deviation of  $1/2$ . Here,  $N$  is the number of the terms considered in the series. It was shown by Fan and Ahmadi that the velocity correlation of the digitally simulated field obtained with  $N = 100$  are in good agreement with the theoretical expression [18]. Equation (6) is in non-dimensional form with the dimensionless quantities given by:

$$u_i^* = \frac{u_i}{u_0}, \quad x_i^* = \frac{x_i}{l_0}, \quad t^* = \frac{t}{l_0 / u_0} \quad (7)$$

Where  $l_0$  and  $u_0$  denote the characteristics length and velocity scales of turbulence.

Normal component of turbulence fluctuations near a wall has a profound effect on the settling rate of bubbles. Therefore, its magnitude must be correctly evaluated for small values of  $y$ . The following expression for the normal velocity fluctuation is used [18]:

$$v' = v'_i (0.0278 y^+)^2 \quad 0 < y^+ < 11 \quad (8)$$

Where  $v'$  the corrected velocity fluctuation in  $y$  direction and

$$y^+ = \frac{y\sqrt{\tau_w/\rho}}{\nu} \quad (9)$$

### C. Lagrangian approach for bubble motion

The motion equation of a spherical particle in a fluid has been derived by Maxey and Riley [19]. For a spherical bubble with radius  $R$ , the equation of motion is given as,

$$\begin{aligned} \rho_b V_b \frac{d\bar{U}_b}{dt} = & V_b(\rho_b - \rho)\bar{g} + V_b \bar{\nabla} p + \frac{1}{2} \rho A_b C_D (\bar{U} - \bar{U}_b) |\bar{U} - \bar{U}_b| + \\ & \frac{1}{2} \rho V_b \left( \frac{d\bar{U}}{dt} - \frac{d\bar{U}_b}{dt} \right) + \frac{1}{2} \rho (\bar{U} - \bar{U}_b) \frac{dV_b}{dt} + \\ & 1.615 \rho \nu^{\frac{1}{2}} d^2 (\bar{U} - \bar{U}_b) \left| \frac{d\bar{U}}{dy} \right|^{\frac{1}{2}} \text{Sgn} \left( \frac{d\bar{U}}{dy} \right) \bar{j} \end{aligned} \quad (10)$$

Here terms with the subscript  $b$  are related to the bubble and those without a subscript are related to carrying fluid.  $U$  and  $U_b$  are fluid and bubble velocity, respectively.  $V_b$  and  $A_b$  are the bubble volume and projected area, which are equal to  $4/3\pi R^2$  and  $\pi R^2$  respectively. The bubble drag coefficient  $C_D$  in equation (10) can be determined by using the empirical equation of Langmuir and Blodgett [20]:

$$\begin{aligned} C_D = & \frac{24}{\text{Re}} (1 + 0.197 \text{Re}^{0.63} + 2.6 \times 10^{-4} \text{Re}^{1.38}) \\ \text{Re} = & \frac{2R|U - U_b|}{\nu} \end{aligned} \quad (11)$$

The physical meaning of each term in the right hand side of equation (10) is as follows. The first term is the buoyancy force. The second term is due to the pressure gradient in the fluid surrounding the particle. The third term is the drag force. The fourth term is the force to accelerate the virtual “added mass” corresponding fluid. The fifth term is the force due to the bubble volume variation, and the last term is the Saffman shear lift force. By dividing both sides of equation (10) to  $\rho V_b$ , the equation for bubble motion becomes:

$$\begin{aligned} \frac{d\bar{U}_b}{dt} = & 2\bar{g} - \frac{3}{\rho} \bar{\nabla} p + \frac{3}{4} \frac{C_D}{R} (\bar{U} - \bar{U}_b) |\bar{U} - \bar{U}_b| + \frac{3}{R} (\bar{U} - \bar{U}_b) \dot{R} + \\ & \frac{1.542}{R} \nu^{\frac{1}{2}} (\bar{U} - \bar{U}_b) \left| \frac{d\bar{U}}{dy} \right|^{\frac{1}{2}} \text{Sgn} \left( \frac{d\bar{U}}{dy} \right) \bar{j} \end{aligned} \quad (12)$$

Where  $(\bar{U} - \bar{U}_b)$  is relative velocity between bubble and fluid which is computed at the centre of bubble.

### D. Improved Spherical Bubble Dynamics Model

The behaviour of spherical bubble in a pressure field is usually described by the Rayleigh-Plesset equation [1]:

$$R\ddot{R} + \frac{3}{2} \dot{R}^2 = \frac{1}{\rho} \left[ p_v + p_g - p - \frac{2\gamma}{R} - \frac{4\mu}{R} \dot{R} \right] \quad (13)$$

Where  $R$  is the time dependent bubble radius,  $\rho$  is the liquid density,  $p_v$  is the vapor pressure,  $p_g$  is the gas pressure inside the bubble,  $p$  is the ambient pressure local to the bubble,  $\mu$  is the liquid viscosity, and  $\gamma$  is the surface tension. For a perfect gas undergoing a polytropic compression, the following relationship relates the gas pressure and the bubble radius:

$$p_g = p_{g0} \left( \frac{R_0}{R} \right)^{3K} \quad (14)$$

Where  $p_{g0}$  and  $R_0$  are the initial gas pressure and bubble radius respectively and  $K$  is the polytropic gas constant. The internal process inside the bubble is assumed to be isentropic. In equation (13) the bubble grows principally in response to a change in the ambient pressure through gaseous expansion and increase in the vapor mass within the bubble. A one-way coupling analysis is adopted here and the effect of the bubble on the liquid is ignored. Equation (13) does not take into account the effect of slip velocity between the bubble and the carrier liquid. To account for this slip velocity, an additional pressure term  $\rho(\bar{U} - \bar{U}_b)^2/4$  is added to the classical Rayleigh-Plesset equation [21]:

$$R\ddot{R} + \frac{3}{2} \dot{R}^2 = \frac{1}{\rho} \left[ p_v + p_g - p - \frac{2\gamma}{R} - \frac{4\mu}{R} \dot{R} \right] + \frac{\rho(\bar{U} - \bar{U}_b)^2}{4} \quad (15)$$

Virtually all liquids contain some dissolved gas. Indeed it is virtually impossible to eliminate this gas from any substantial liquid volume. If the nucleation bubble contains some gas, then the pressure in the bubble is the sum of the partial pressure of this gas,  $p_g$ , and the vapor pressure. Hence the equilibrium pressure in the liquid is:

$$p = p_V + p_G - \frac{2\gamma}{R} \quad (16)$$

Where  $R$  is the time dependent bubble radius,  $p_v$  is the vapour pressure,  $p_g$  is the gas pressure inside the bubble,  $p$  is the ambient pressure local to the bubble,  $\gamma$  is the surface tension. In the context of cavitation flow, it is appropriate to assume that the microbubble of radius  $R_0$  is in equilibrium at  $t = 0$  in the fluid at pressure  $p$  so that:

$$p_{G0} = p - p_V(T_\infty) - \frac{2\gamma}{R_0} \quad (17)$$

### E. Collision model

Analysis of bubbles collision in this study is based on the hard sphere collision model developed by Hoomans et al with the following assumptions [11]:

- Two-dimensional movement is considered.
- Bubbles are spherical and quasi-rigid.

- Collisions are binary and instantaneous with point contact.
  - Interaction forces are impulsive and all other forces are negligible during collision.
  - The effects of the rotation of bubbles are neglected.
- If a and b are discrete-phase collision pairs, the velocities of a and b after a collision are given as:

$$\begin{aligned} u_{a1} &= \frac{px}{m_a} + u_{a1}, & v_{a1} &= \frac{py}{m_a} + v_{a1} \\ u_{b1} &= \frac{px}{m_b} + u_{b1}, & v_{b1} &= \frac{py}{m_b} + v_{b1} \end{aligned} \quad (18)$$

Where  $u$  and  $v$  are components of velocity and subscripts 1 and 2 refer, respectively, to before and after collision:

$$\begin{aligned} px &= -\mu * py * \text{sgn}(u_{a1} - u_{b1}) && \text{For sliding case} \\ px &= -(u_{a1} - u_{b1}) / B && \text{For stick case} \\ py &= -\frac{(1+e)(v_{a1} - v_{b1})}{C} \end{aligned} \quad (19)$$

Here,  $e$  is the restitution coefficient;  $\mu$  is the friction coefficient, and  $B$  and  $C$  are collision constants given as:

$$B = \frac{1}{m_a} + \frac{1}{m_b} + \frac{R_a^2}{I_a} + \frac{R_b^2}{I_b}, C = \frac{1}{m_a} + \frac{1}{m_b} \quad (20)$$

Where  $R_a$  and  $R_b$  are, respectively, the radius of particles  $a$  and  $b$ , and  $I_a$  and  $I_b$  are the corresponding moments of inertia given by:

$$I_a = \frac{2}{3} m_a R_a^2, I_b = \frac{2}{3} m_b R_b^2 \quad (21)$$

The slip and stick conditions during the collision are determined according to

$$\begin{aligned} |u_{a1} - u_{b1}| &\geq \mu B py && \text{Sliding} \\ |u_{a1} - u_{b1}| &< \mu B py && \text{Sticking} \end{aligned} \quad (22)$$

In this study, friction coefficients of 0.02 and restitution coefficients of 0.2 are used [14].

### III. VALIDATION OF COLLISION MODEL

To validate the algorithm used in the bubbles collision, a modified version of a test used by Schmidt and Rutland was performed [22]. This test compares the number of collisions predicted by a specified collision model with the number of collisions obtained from the analytical or mathematical expression for the integral of the collision probability.

The domain for this test consisted of a two-dimensional,  $4 \times 4$  grid with solid walls. The width of domain is unit. The  $N_p$  particles uniformly distributed throughout the domain. The radiuses of particles were uniformly distributed from the

interval 0 to  $5 * 10^{-7}$  m. Likewise, the  $x$ -component of the particle velocities were sampled uniformly from the interval 0 to 1 m/s, and the  $y$ -component was set to zero. A single time step of  $10^{-4}$  s was used.

Over a single time step, the number of predicted particle collisions was counted in each collision cell and totalled. The number of predicted particles collision was then compared to the expected number of collisions in each cell, calculated from the following analytical or mathematical expression [22]:

$$M_{theory} = \sum \frac{7\pi\Delta t v_{\max}^2 r_{\max}^2 N_p}{36\forall} \quad (23)$$

Where,  $N_p$ ,  $\forall$  and  $M$  are the number of particles in the collision cell, volume of each and number of collision, respectively. The relative error was then calculated using

$$\varepsilon_{rel} = \frac{|M_{theory} - M_{predicted}|}{M_{theory}} \quad (24)$$

Since the collision model is highly stochastic in nature, this relative error was averaged over forty independent runs in order to minimize random effects. Results are shown in Fig. 1. A good agreement between the present computation and analytical result is achieved.

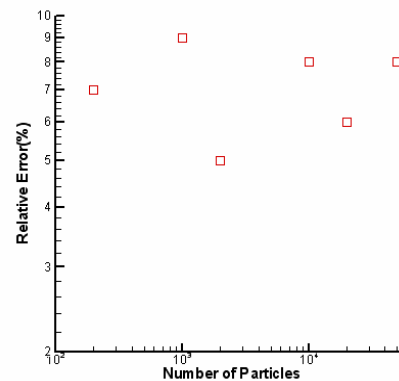


Fig 1: Relative error of collision model compared with the analytical solution

### IV. NUMERICAL SOLUTION PROCEDURE

Since the bubble is considered very small, the interaction between bubble and fluid-phase can be ignored. The Navier-Stokes equation for incompressible flow is solved. The SIMPLEC algorithm is used for coupling the velocity and pressure. RSTM model is used to model turbulence. Maximum relative error is considered smaller than 0.0005. A grid with about 20,000 cells is generated for analyzing the flow. The grid independency is checked in order to make sure that the grid numbers is sufficient and has enough accuracy. The boundary condition of fully developed flow is used for the channel inlet and outlet. Fig. 2 illustrates the boundary conditions used for numerical simulation. Sticking condition for the bubbles is considered in the walls. It is assumed that the bubbles are eliminate from the simulation when collide to

wall of channel.

The Gaussian random field model is used to simulate the instantaneous fluctuation of velocity. Velocity profile in  $x$  direction with considering fluctuations at a section of the channel is shown in Fig. 3.

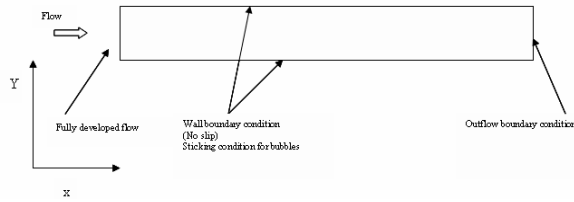


Fig. 2: Solution domain and boundary conditions

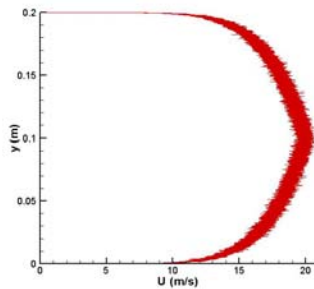


Fig. 3: Instantaneous velocity profile in  $x$ -direction by using Kraichnan model

The position and velocity of bubbles are obtained using Eq. (11). A fourth-order Runge- Kutta method is used to solve this equation. Fluid velocity in centre of bubbles is used to find the bubbles slip velocity. In the hard-sphere approach, a sequence of binary collisions is processed by using one collision at a time. A collision list has to be compiled and a corresponding collision time needs to be stored. This requires a considerable CPU time. In order to reduce the required CPU time, an algorithm is used. In this algorithm, a new grid for discrete phase is generated again. For each bubble, a list of neighbor bubble is stored and only bubbles that are in the same or neighbour cell are checked for possible collision. For this purpose, a  $0.5\text{ cm}$  rectangular grid is used for the bubbles. Several fluid control volumes are taken to represent an elementary volume in the Eulerian coordinate system. Each bubble in the fluid control volumes represents a bubble control volume. Every bubble within the fluid control volumes (bubble  $i$ ) and its adjacent four fluid control volumes are included in a list, so that this collision searching is only limited to the bubble  $i$  located and its nearest four neighbor fluid control volume. After obtaining collisions, the shortest collision time of each bubble is determined. If the overall shortest collision time is smaller than the time-step of gas-phase, the bubble positions are updated by this shortest overall collision time. In the next step, new radius of bubbles is obtained by using the Rayleigh-Plesset equation. The mass of micro bubbles is considered fixed in the simulation. A flow chart of numerical solution procedure is indicated in Fig. 4.

V. RESULTS AND DISCUSSION

Number of 1000 and 1500 micro bubble are released in the near wall ( $0 < y^+ < 40$ ) and their trajectory with considering collision are investigated. Initial velocity of micro bubble is  $20\text{ m/s}$ . Initial radius of micro bubbles is randomly considered between 1 and 10 micron.

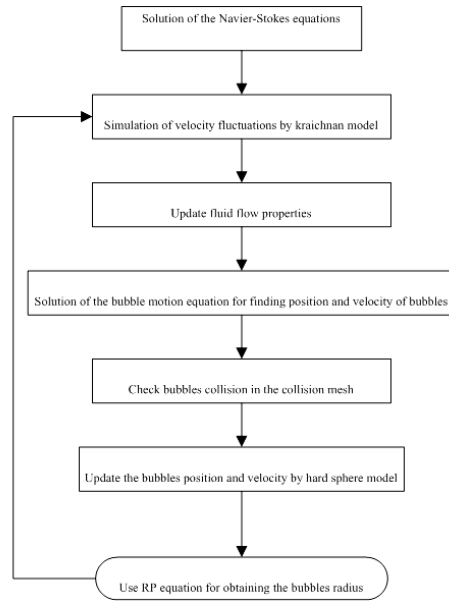


Fig. 4: Flow chart of numerical solution

Cavitation occurs by sudden expansion and the volumetric oscillation of bubble nuclei in the water due to the ambient pressure change. Therefore, Micro bubbles are initial nuclei for formation of the hydrodynamic cavitation. These micro bubbles convert to cavitation bubble when they reach to the low-pressure regions. In these regions, abrupt growth is created and bubbles radius enlarges suddenly. Cavitation could be predicted with tracing the microbubbles' trajectory. Fig. 5 shows micro bubbles trajectory in length of the channel. It is shown that a few of micro bubbles are able to separate from boundary points of the channel wall. If these micro bubbles situate in appropriate location and pressure decrease enough, they can grow and convert to cavitation bubbles.

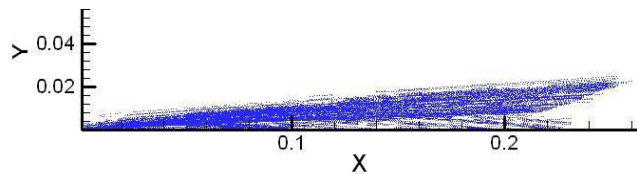


Fig. 5: Micro bubbles trajectory in the channel (The initial bubble radius is randomly considered between 1 and 10 micron and located randomly in  $0 < y^+ < 40$ )

The radius of bubble changes along the channel length due to pressure changes. Radius variation of a bubble in a time interval is indicated in Fig 6. Radius of bubbles is affected by pressure gradient and surface tension forces. The variation of bubble radius is oscillating. The interaction of

surface tension and external pressure causes this oscillating variation of radius.

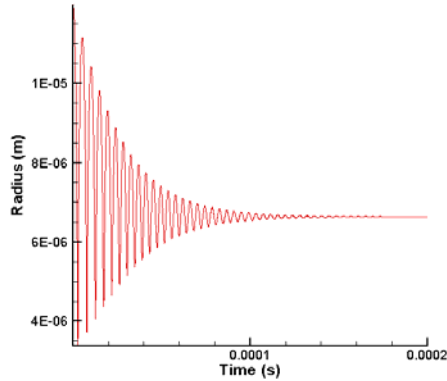


Fig. 6: Radius variation of a micro bubble as function of time (Initial radius of bubble is  $10\ \mu\text{m}$ )

The dispersion of microbubbles along the channel is presented in Fig 7. The initial bubble radius is randomly considered between 1 and 10 micron. The bubbles are initially located randomly in  $0 < y^+ < 40$ . The distribution of bubbles is similar to turbulent velocity profile. But, this distribution changes after a few time steps. This change of distribution could be related the change of bubbles' volume and the buoyancy forces.

The bubbles settle by their weight and velocity fluctuations near wall. As indicated in Fig. 8, many the micro bubbles collide to wall. Micro bubbles settle in start of movements rapidly. Then, the rate of settling of micro bubbles decrease gradually. The figure shows comparison of results with 1000 and 1500 micro bubble for number of settled bubbles. The shape of both curves is same and with increasing number of bubbles, rate of settling increase, as expected. The velocity fluctuations of fluid near wall can cause increasing drag force acting on the micro bubbles in  $y$  direction, and the bubbles may collide to wall and settle.

Because micro bubbles are very small, the probability of their collision in a large domain is low. As indicated in Fig. 9, since released micro bubbles are located in the vicinity each other first, the rate of collision is more. As indicated in the figure, number of collisions does not decrease with increasing time gradually. It is shown that the rate of collision increase in this time interval sometime. This can occur because of random nature of velocity fluctuations. The velocity fluctuation can cause aggregation of micro bubbles and therefore increasing the rate of collision.

Comparison of results with 1000 and 1500 micro bubble for rate of collision is also shown in the figure. Since the bubbles are released from near the wall,  $0 < y^+ < 40$ , collision of the micro bubbles together may cause settling of the bubbles. Therefore, rate of collision also affect on rate settling, increasing of rate collision increase settling of bubbles. At beginning of simulation, rate of collision is more than other times. This may increase rate of settling.

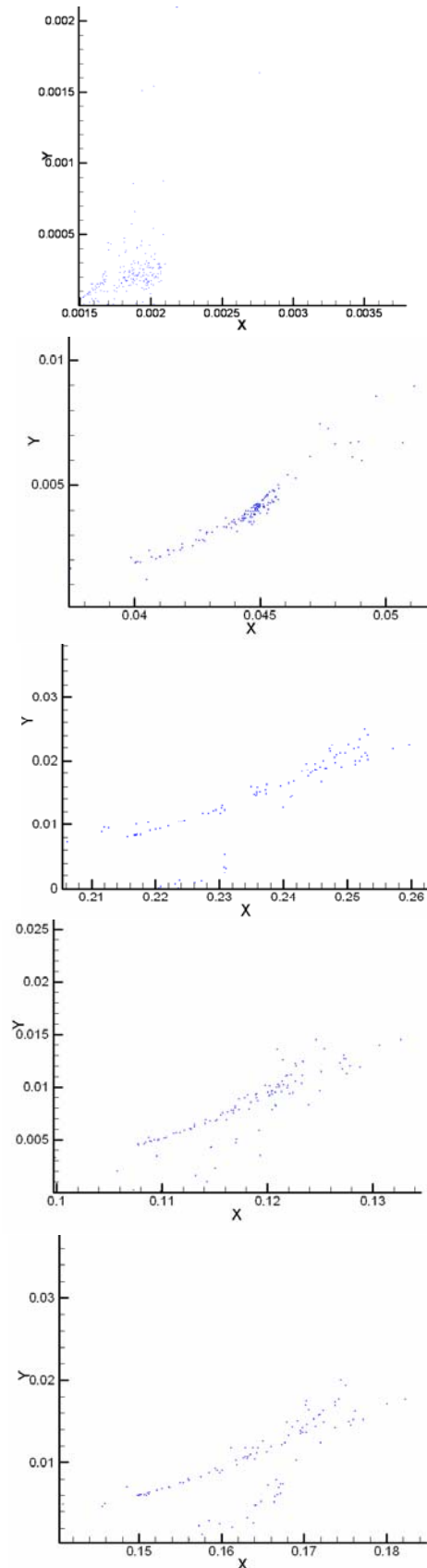


Fig. 7: The location of moving micro bubbles in different sections of the channel

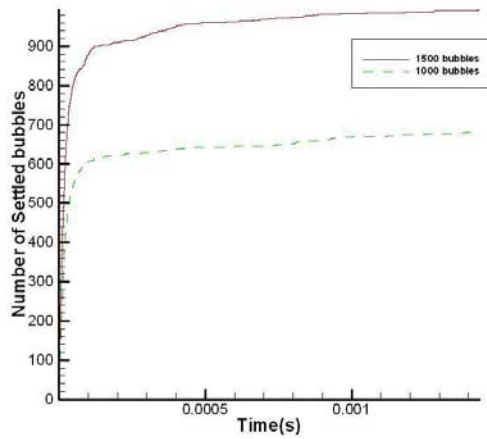


Fig. 8: Comparison of number of settled bubbles as function of time in the channel for 1000 and 1500 micro bubble

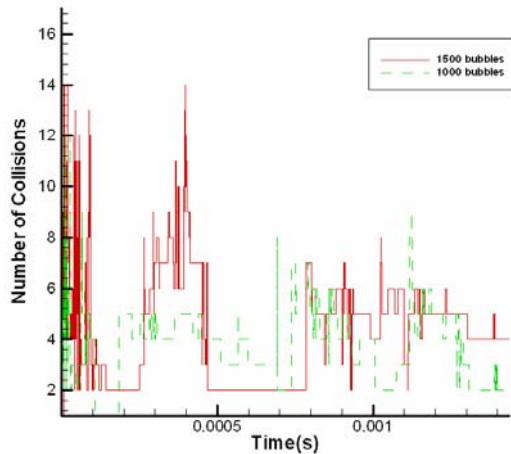


Fig. 9: Comparison of collision as function of time in the channel for 1000 and 1500 micro bubble

## VI. CONCLUSIONS

In this paper, the micro bubbles trajectory with considering collisions in the channel, that has simple geometry and low computational cost, is studied. The Eulerian – Lagrangian approach is used to analyze two-phase flow. A two-dimensional is used to simulate flow field. The RSTM is used to simulate turbulent stresses. The components of instantaneous fluctuation velocity are simulated using the Gaussian random field model. Analysis of bubbles collision is done using hard sphere collision model. For validation of the collision model is used from a test case. The numerical results have good agreement with the analytical results. Trajectories of micro-bubbles in the near wall region were investigated, and the rate of collisions and bubble settling rate were studied.

This method can be used to predict and estimate cavitation using micro bubbles trajectory in industrial applications.

## APPENDIX

### Nomenclature

- $R$  : Bubble radius  
 $R_0$  : Bubble initial radius  
 $\dot{R}$  : Radius surface velocity  
 $\ddot{R}$  : Radius surface acceleration  
 $Re$  : Reynolds number  
 $t$  : Time  
 $U$  : Relative velocity (bubble-fluid)  
 $U_f$  : Fluid velocity  
 $U_b$  : Bubble velocity

### Greek letters

- $\nu$  : Kinematic viscosity  
 $\rho$  : Density

### Subscripts

- $f$  : Fluid  
 $b$  : Bubble  
 $G$  : Gas

## REFERENCES

- [1] M.S. Plesset, "Dynamics of Cavitation Bubbles" *Journal of Applied Mechanics*, Vol. 16, 1948, pp. 228-231.
- [2] R.S. Meyer, M.L. Billet, J.W. Holl, "Freestream Nuclei and Traveling Bubble Cavitation", *ASME J. Fluids Eng.*, Vol. 114, 1992, pp. 672-679.
- [3] C. T. Hsiao, L. L. Pauley, "Study of Tip Vortex Cavitation Inception using Navier-Stokes Computation and Bubble Dynamics Model", *ASME J. Fluids Eng.*, 121(1), 1999, pp. 198-204.
- [4] J. E. Johnson, T. Hsieh, "the Influence of the Trajectories of the Gas Nuclei on Cavitation Inception", *Sixth Naval Hydrodynamics Symposium*, 2000, pp. 163-182.
- [5] K. J. Farrell, "Eulerian/Lagrangian analysis for the prediction of cavitation inception", *International Symposium on Cavitation (CAV2001)*, 2001.
- [6] A. Raoufi, M. Shams, R. Ebrahimi, G. Ahmadi, "Numerical Simulation of Bubble Motions in a Gate Slot", *Engineering Letters*, Vol. 15 Issue 2, 2007, pp. 376-381.
- [7] J. K. Dukowicz, "A particle-fluid numerical model for liquid sprays", *J. Comput. Phys.*, Vol.35, 1980, pp. 229-253.
- [8] P. J. O'Rourke, "Collective Drop Effects on Vaporizing Liquid Sprays", *Department of Mechanical and Aerospace Engineering, Princeton University*, 1981.
- [9] M. Sommerfeld, G. Zivkovic, "Recent advances in the numerical simulation of pneumatic conveying through pipe systems, *Computational Methods in Applied Sciences*, 1992, pp. 201-212.
- [10] Y. Tsuji, T. Kawaguchi, T. Tanaka, "Discrete particle simulation of two dimensional fluidized bed", *Powder Technology*, Vol. 77, 1993, pp.79-87.
- [11] B. P. B. Hoomans, J. A. M. Kuipers, W. J. Briels, "Discrete particle simulation of bubble and slug formation in a two-dimensional gas fluidized bed: a hard-sphere approach", *Chemical Engineering Science*, 51, 1996, pp. 99-118.
- [12] M. J. V. Goldschmidt, R. Beetstra, J. A. M. Kuipers, "Hydrodynamic modelling of dense gas-fluidized beds: Comparison of the kinetic theory of granular flow with 3D hard-sphere discrete particle simulations", *Chemical Engineering Science*, 57, 2002, pp. 2059-2075.
- [13] H. Lu, S. Wang, Y. Zhao, L. Yang, D. Gidaspow, J. Ding, "Prediction of particle motion in a two-dimensional bubbling fluidized bed using discrete hard-sphere model", *Chemical Engineering Science*, 60, 2005, pp. 3217 - 3231.

- [14] X. Zhang, G. Ahmadi, "Eulerian-Lagrangian simulations of liquid-gas-solid flows in three-phase slurry reactors", *Chemical Engineering Science*, Vol.60, 2005, pp. 5089 – 5104.
- [15] B.E. Launder, G.J. Reece, W. Rodi, "Progress in the development of a Reynolds stress turbulent closure", *J Fluid Mech.*, 68, 1975, pp.537-548.
- [16] R.H. Kraichnan, "Diffusion by Random Velocity Field", *Physics of Fluids*, Vol.13, 1970, pp. 441-465.
- [17] M. R. Maxey, "The Gravitational Settling of Aerosol Particles in a Homogenous Turbulence and Random Flow Field", *J. Fluid Mech.*, Vol. 174, 1987, pp. 441-465.
- [18] F. G. Fan, G. Ahmadi, "Analysis of Particle Motion in the Near-Wall Shear Layer Vortices- Application to the Turbulent Deposition Process", *J. Colloid and Interface Sci.*, Vol. 172, 1995, pp. 263-277.
- [19] M. R. Maxey, J. J. Riley, "Equation of Motion for a Small Rigid Sphere in a Nonuniform Flow", *Phys. Fluids*, Vol. 26. No. 4, 1983, pp. 883 – 889.
- [20] I. Langmuir, K. B. Blodgett, "A Mathematical Investigation of Water Droplet Trajectories", U.S. Army Air Force Tech. Rep. No. 5418, 1945.
- [21] C. Brennen, "Cavitation and Bubble Dynamics", Oxford University press, 1995.
- [22] D.P. Schmidt, C.J. Rutland, "A New Droplet Collision Algorithm", *J. of Computational Physics*, Vol. 164, 2000, pp. 62-80.